Energy & Environmental Science

Cite this: DOI: 10.1039/c0ee00793e

www.rsc.org/ees

COMMUNICATION

Nano-structured textiles as high-performance aqueous cathodes for microbial fuel cells†

Xing Xie,[a] Mauro Pasta,[bc] Liangbing Hu,[b] Yuan Yang,[b] James McDonough,[b] Judy Cha,[b] Craig S. Criddle*[a] and Yi Cui*[b]

Received 20th December 2010, Accepted 1st February 2011
DOI: 10.1039/c0ee00793e

A carbon nanotube (CNT)–textile–Pt cathode for aqueous-cathode microbial fuel cells (MFCs) was prepared by electrochemically depositing Pt nanoparticles on a CNT–textile. An MFC equipped with a CNT–textile–Pt cathode revealed a 2.14-fold maximum power density with only 19.3% Pt loading, compared to that with a commercial Pt coated carbon cloth cathode.

Microbial fuel cell (MFC) technology is promising for wastewater treatment because it enables recovery of clean electric energy as wastewater organic matter is oxidized.[1–4] The preferred oxidant is the oxygen in air because it is cheap and readily available,[5,6] but the efficiency of oxygen reduction is constrained by operating conditions (low oxygen solubility, temperature and mostly neutral pH).[5,7,8] Consequently, cathode performance often limits MFC power output.[7,9] In addition, the cathode usually accounts for the greatest part of the capital cost of a MFC, due to the use of expensive metal catalysts, such as Pt.[10] Improving cathode performance and driving down cathode costs are therefore critical.[5]

According to the different cathode configurations, MFCs are classified into two categories: aqueous-cathode MFCs and air-cathode MFCs. In an aqueous-cathode MFC, the cathode is immerged in an electrolyte purged with air, thus oxygen dissolved in the electrolyte works as an electron acceptor,[7] while for an air-cathode MFC, one side of the cathode is directly exposed to air and gas phase oxygen is reduced.[4] A common opinion is that aqueous-cathode MFCs do not perform as well as air-cathode MFCs.[2] However, most of the previous studies on aqueous-cathode MFCs employed cathodes prepared by coating a carbon supported catalyst paste onto a carbon cloth (CC) substrate.[7,11–15] This cathode configuration, widely used in chemical fuel cells, is actually designed for oxygen reduction in the gas phase. An aqueous-cathode MFC may also achieve high performance if the cathode can be well designed for reduction of oxygen dissolved in the electrolyte. In the case of an air-cathode MFC where an aqueous electrolyte is only on the anode side, the separator or separator/cathode composite needs to be strong enough to withstand the hydrostatic pressure. This is a challenge for air-cathode MFCs at large scales. However, the requirements on mechanical properties are much lower for the separator in an aqueous-cathode MFC because both sides of the separator are filled with aqueous electrolyte. Moreover, some modified MFC

[a]*Department of Civil and Environmental Engineering, Stanford University, Stanford, California, 94305, USA. E-mail: ccriddle@stanford.edu; Tel: +1-650-723-9032*
[b]*Department of Materials Science and Engineering, Stanford University, Stanford, California, 94305, USA. E-mail: yicui@stanford.edu; Fax: +1-650-725-4034; Tel: +1-650-723-4613*
[c]*Dipartimento di Chimica Inorganica, Metallorganica e Analitica "Lamberto Malatesta", Università degli Studi di Milano, Via Venezian 21, 20133 Milan, Italy*

† Electronic supplementary information (ESI) available: Experimental details, XRD pattern, and CV curves for ECAS area measurements. See DOI: 10.1039/c0ee00793e

Broader context

Microbial fuel cells (MFCs) can recover energy from waste due to the catalytic activity of microorganisms, alleviating both energy and environmental problems. The concept of harvesting electricity from domestic wastewater by MFCs has been demonstrated. However, poor performance and the high capital cost of the catalysts required in cathodes hinder the scaling-up of MFCs to real applications. While most studies focus on air-cathodes, aqueous-cathodes are also important configurations and are essential for some modified MFC technologies, such as microbial desalination cells and microbial electrolysis cells. However, the widely used cathode in aqueous-cathode MFCs, carbon cloth coated with catalyst paste, is actually designed for oxygen reduction in gas phase. Therefore, it is a significant advance that we report this CNT–textile–Pt composite designed as an aqueous-cathode for the first time and that an MFC equipped with the CNT–textile–Pt achieved both an increase in power density and a decrease in Pt loading at the same time. Moreover, the synthesis process of CNT–textile–Pt is simple and scalable. Thus, this CNT–textile–Pt is promising to function as cathodes for large scale aqueous-cathode MFCs and other modified MFC technologies. Additionally, the novel design of our cathode structure is also applicable in other fuel cells requiring aqueous cathodes.

technologies prefer an aqueous-cathode. For example, in a microbial desalination cell, the catholyte is essential for collecting the cations, *e.g.* Na^+, transported through the cation exchange membrane from the salt water.[16] Therefore, while most current studies focus on optimizing air-cathodes,[17–19] improving the aqueous-cathode is also meaningful.

To catalyze oxygen reduction, catalysts must have simultaneous access to oxygen, electrons, and electrolyte.[20] The catalytic surface area having this triple-access, termed as electrochemically active surface (ECAS) area, is directly related to the cathode performance.[21] In a conventional air-cathode, the carbon support, *e.g.* carbon black, provides the electron pathway, while a Nafion membrane works as the electrolyte, providing proton conduction. The porous structure of the composite electrode possesses high interfacial surface area with the gas phase to facilitate oxygen transfer.[20–22] In an aqueous-cathode system, because oxygen is dissolved in the aqueous electrolyte, the structure design is much easier. However, an open porous structure, with pore sizes larger than those of conventional air-cathodes, is preferred for easier access of the electrolyte.

We have recently synthesized a highly conductive single walled carbon nanotube (CNT)–textile composite by conformally coating a microscale porous CNT layer (~200 nm thick) on textile fibers with diameters around 20 μm[23] as well as paper fibers.[24] The microscale pores are formed in the space between CNTs with diameters ~100 nm. The space between textile fibers for macroscale pores is ~100 μm. The CNT–textile provides high specific surface area and has been studied as high performance electrodes in supercapacitors[23,25] and MFC anodes.[26] In this study, we propose a new composite cathode prepared by further depositing Pt nanoparticles onto the CNT–textile substrate using an electrochemical method. The schematic of this CNT–textile–Pt composite is shown in Fig. 1. For this CNT–textile–Pt cathode, the electrochemical deposition method guarantees the electronic pathway to all of the catalyst,[20] while the open and macroscale porous CNT–textile provides high specific catalyst–electrolyte interfacial surface area.[23] These properties make the CNT–textile–Pt cathode distinct from other types of conventional cathodes.

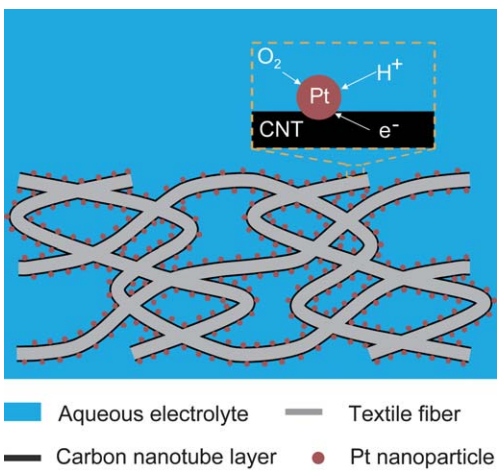

Fig. 1 Schematic of the CNT–textile–Pt composite in aqueous electrolyte. While the electrochemical deposition method guarantees electronic access to the Pt, the open and macroscale porous structure of the CNT–textile facilitates the contact between the Pt and the aqueous electrolyte containing oxygen.

The scanning electron microscopy (SEM) image of the plain surface of CNT–textile is shown in Fig. 2a. The randomly intertwined textile fibers form an open macroscale porous structure. The conformally coated CNTs make the CNT–textile highly conductive, with a sheet resistance of 4 Ω sq^{-1}.[23] An acid treatment process (glacial acetic acid, 2 hours) increases the hydrophilicity of the CNT–textile and creates oxygen-rich functional groups on the originally inert CNT surface acting as nucleating sites for Pt deposition.[27,28] Then the electrochemical deposition process was performed in a flask containing chloroplatinic acid (H_2PtCl_6, 0.019 M) and hydrochloric acid (HCl, 0.6 M) as electrolyte, by fixing the potential of CNT–textile at −0.6 V *vs.* a double junction Ag|AgCl|KCl (3.5 M) reference electrode (RE) and limiting the charge at 600 mC.[27] Fig. 2b shows the SEM image of the CNT–textile–Pt composite. Because Pt particles were deposited by electrochemical reduction, only the sites with electronic access were covered with Pt particles. Therefore, the electron pathways to all the catalysts are guaranteed. As shown in Fig. 2b, the deposited Pt particles are uniformly distributed along the CNT–textile backbone making the Pt particles easy to access by the electrolyte containing oxygen and proton. Thus, in CNT–textile–Pt, almost every Pt particle has the triple-access for oxygen reduction.

The performance of the CNT–textile–Pt composite as an aqueous cathode was compared with a commercial CC cathode with Pt

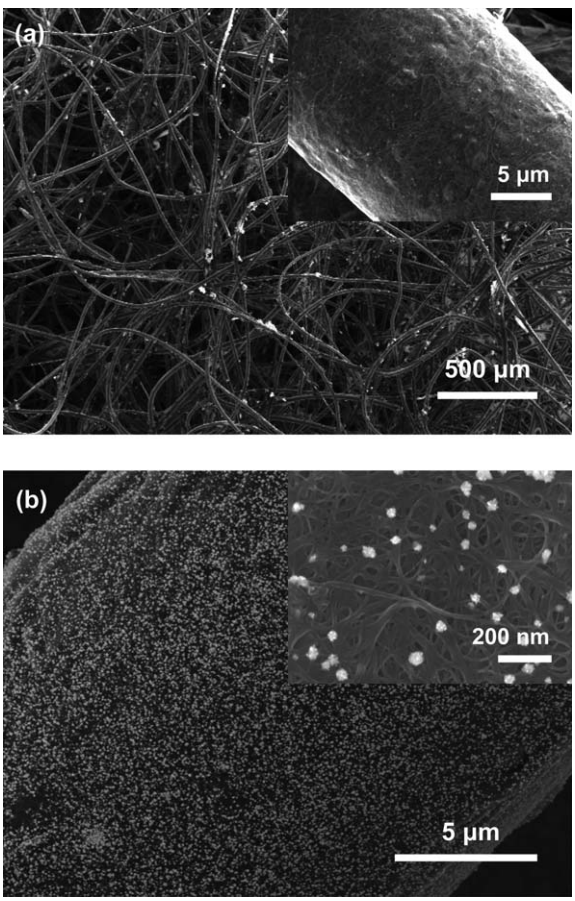

Fig. 2 (a) SEM image of the surface of plain CNT–textile, displaying the macroscale porous structure and the conformal CNT coating. (b) SEM image of the CNT–textile–Pt, showing the uniform distribution of Pt nanoparticles.

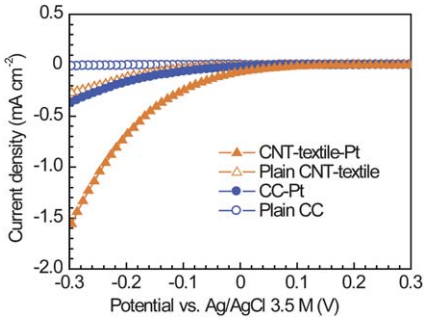

Fig. 3 LSV results showing the oxygen reaction activities of different cathodes. Current densities were normalized by the projected surface area of the cathode (2 cm^2).

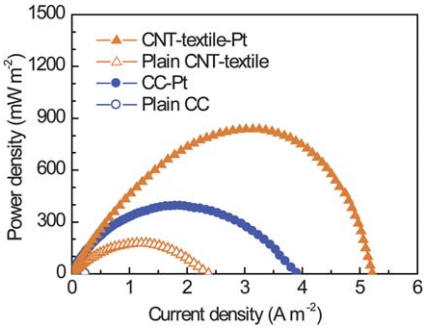

Fig. 4 Polarization curves of MFCs with different cathodes. Power and current densities are normalized by the projected surface area of electrodes (2 cm^2).

catalyst (CC–Pt), which was prepared by a general painting method[7,11–15] (Fuel Cell Earth, USA, Fig. S1†). The oxygen reduction activity of the cathode samples (1 cm × 1 cm) was characterized by applying linear staircase voltammetry (LSV) at a step-sweep rate of 10 mV per 10 seconds from 0.3 to −0.3 V *vs.* a double junction Ag|AgCl|KCl (3.5 M) RE. The electrolyte was a phosphate buffer solution saturated with oxygen under ambient pressure and temperature, in order to simulate the working condition in aqueous-cathode MFCs.[7] As shown in Fig. 3, the CNT–textile–Pt cathode generates much larger reduction currents than those of the CC–Pt, indicating the superior oxygen reduction activity. While oxygen reduction by the plain CC without Pt is almost negligible, the plain CNT–textile without Pt also reveals certain oxygen reduction activity, resulting from the catalytic activity of CNTs that has been reported by several studies.[20,21] However, the catalytic activity of CNTs alone is much lower than that of Pt. In order to investigate the long term stability of the CNT–textile–Pt cathode, cyclic voltammetry (CV) measurements were performed at a scan rate of 10 mV s^{-1} between −0.5 and 0.5 V *vs.* a double junction Ag|AgCl|KCl (3.5 M) RE in the same electrolyte as that applied in the LSV tests. The result shows that the oxygen reduction activity of the CNT–textile–Pt does not decay after 2000 cycles (Fig. S2†).

Cathode samples were investigated in an H-shaped two-chamber MFC with a CNT–textile anode (1 cm × 1 cm).[26] The MFC was inoculated with domestic wastewater and had been operated for 6 months to obtain mature biofilms on the anode. Maximum power densities of the MFCs equipped with different cathodes were determined from the polarization curves measured under a step-sweep rate of 10 mV per 10 seconds starting from the OCV value. As shown in Fig. 4, in accordance with the results of oxygen reduction, the CNT–textile–Pt cathode shows much better performance than the CC–Pt cathode with the same projection area of electrode. The maximum power density of the MFC with the CNT–textile–Pt cathode is 837 mW m^{-2}, 2.14 times of that achieved by the MFC with the CC–Pt cathode (391 mW m^{-2}). The MFC prepared with the plain CNT–textile cathode also generates a maximum power density of 177 mW m^{-2}. Even after removing this contribution of the CNTs, the CNT–textile–Pt cathode still shows 1.7 times better performance than the CC–Pt cathode, which indicates that the Pt in CNT–textile–Pt provides greater catalytic activity. The maximum current density achieved by the CNT–textile–Pt cathode is 5.2 A m^{-2}, much higher than the value reported in a recently published paper (0.1 A m^{-2}).[29] They also applied a CNT–Pt composite, synthesized by filtering a dispersion of CNTs and Pt nanoparticles through a membrane, as the cathodes for MFCs. However, different from the CNT–textile–Pt cathode, their CNT–Pt cathode did not possess a macroscale porous structure and the electronic pathway to Pt nanoparticles was not assured.

Several approaches have been applied to characterize the CNT–textile–Pt cathode samples. Pt loadings were determined by an IRIS advantage inductively coupled plasma atomic emission spectroscopy (ICP-AES) system. The Pt loading of CNT–textile–Pt was controlled by the charge applied during electrochemical deposition. However, only part of the applied charge (15.9% out of 600 mC in this study), defined as coulombic efficiency (CE), is effective for Pt deposition.[27] Some of the electron loss may be due to hydrogen evolution on the surface of Pt nanoparticles.[27] As shown in Table 1, the Pt loading of the CNT–textile–Pt cathode is very little (0.048 mg cm^{-2}) while the commercial CC–Pt cathode (0.249 mg cm^{-2}) is ~five times of our loading. While many studies have been focused on use of alternative catalysts, such as activated carbon, stainless steel, Ni, Fe, Co, Mn, and Cu,[6,8,30–34] decreasing Pt loading in our CNT–textile–Pt provides a direct approach to reduce the capital cost of the cathode. Two more CNT–textile–Pt samples with even lower Pt loadings (0.008 mg cm^{-2} and 0.002 mg cm^{-2}) were synthesized by further decreasing the applied charges to 200 mC and 100 mC, respectively. The maximum power densities of the MFCs equipped with these two cathodes are reduced from 837 mW m^{-2} to 559 mW m^{-2} and 205 mW m^{-2}, respectively (Fig. S3†). The CNT–textile–Pt with only 3.2% Pt loading compared to that of the commercial CC–Pt cathode still achieved a 43% higher power density (559 mW m^{-2} *vs.* 391 mW m^{-2}).

In Fig. 2b, the particle sizes of Pt vary from several nanometres to less than 100 nm. However, the bright dots displayed in the scanning

Table 1 Characterization of CNT–textile–Pt cathodes compared with CC–Pt

	CNT–textile–Pt	CC–Pt
Pt loading/mg cm^{-2}	0.048	0.249
Average size of Pt nanoparticles/nm	9.2	2.6
Theoretical surface area[a]/cm^2 Pt per cm^2 electrode	14.5	262.5
Electrochemically active surface area[b]/cm^2 Pt per cm^2 electrode	7.79	0.92
Surface area utilization efficiency[c] (%)	53.6	0.4

[a] Calculated from Pt loading and average particle size. [b] Obtained from electrochemical measurement. [c] Ratio of electrochemically active surface area to theoretical surface area.

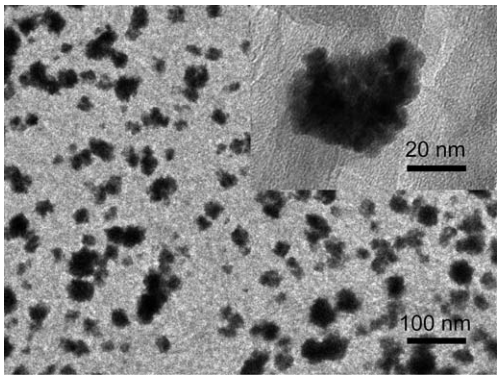

Fig. 5 TEM image showing clusters of Pt particles deposited on the CNT–textile surface.

micrographs are actually clusters of several Pt nanoparticles with smaller sizes (Fig. 2b, inset), an observation confirmed by transmission electron microscopy (TEM) (Fig. 5). The average sizes of Pt particles on different electrodes were calculated by Debye Scherrer equation, based on the X-ray Diffraction (XRD) test results (Fig. S4†),[27,28] and the results are shown in Table 1. With the average particle sizes and total Pt loading, the theoretical overall Pt surface area can be estimated. As shown in Table 1, the CNT–textile–Pt has less theoretical Pt surface area (14.5 cm^2 Pt per cm^2 electrode) than the CC–Pt (262.5 cm^2 Pt per cm^2 electrode) due to the lower mass loading and larger particle sizes. However, the CNT–textile–Pt has much larger ECAS area (7.79 cm^2 Pt per cm^2 electrode, *vs.* 0.92 cm^2 Pt per cm^2 electrode for CC–Pt), determined by an electrochemical method, in which the ECAS area is proportional to the hydrogen adsorption–desorption capability of the electrode (Fig. S5†).[21] Because the ECAS area is more relevant to the catalytic activity, these results explain the different MFC performances achieved by the two cathodes. Comparing the surface area utilization efficiency calculated from the ratio of ECAS area to the theoretical surface area, CNT–textile–Pt is two orders better than the CC–Pt (53.6% *vs.* 0.4%), suggesting that our CNT–textile–Pt cathode is designed well. The significant improvement is due to several reasons: (1) CNT–textile–Pt provides direct electronic pathways for all the Pt particles while CC–Pt has isolated Pt particles where no electronic pathways are formed;[21] (2) CNT–textile–Pt provides macroscale pores for the fast access of electrolyte although CC–Pt has some Pt particles located in small or closed-end pores that are not accessible for the electrolyte; (3) glacial acetic acid treatment in CNT–textile–Pt makes the surface hydrophilic for electrolyte wetting while the hydrophobic surface of the CC–Pt hinders the electrode–electrolyte contact.

CC is also a conductive and porous electrode material, although the carbon fibers are bundled more compactly and the space between fibers is less than that between the CNT–textile fibers.[26] We applied Pt electrochemical deposition on some commercial CC electrodes (Fuel Cell Earth, USA) following the same procedure as described before. The SEM image (Fig. S6†) shows that Pt nanoparticles are also uniformly deposited on the carbon fibers. Testing these cathodes in the same MFC, a maximum power density of 466 mW m^{-2} was achieved when the Pt loading is 0.008 mg cm^{-2}. This performance is not as good as that achieved by the CNT–textile–Pt with similar Pt loading (559 mW m^{-2} with a Pt loading of 0.008 mg cm^{-2}) but much better than that of the commercial CC–Pt cathode (391 mW m^{-2} with a Pt loading of 0.249 mg cm^{-2}). The results confirm that the superior performance of the CNT–textile–Pt cathode is mainly due to the effective design of the cathode structure and the improved catalyst loading technique, while the catalytic activity of CNTs further enhanced the performance.

In summary, a new CNT–textile–Pt cathode especially designed for aqueous-cathode MFCs was obtained by electrochemically depositing Pt nanoparticles on a macroporous CNT–textile substrate. This CNT–textile–Pt cathode shows two orders higher surface area utilization efficiency than that of a commercial CC–Pt cathode. An MFC equipped with the CNT–textile–Pt cathode achieves a higher power density (2.14-fold) with lower Pt loading (19.3%). Moreover, the synthesis process of CNT–textile–Pt is simple and scalable. Thus, CNT–textile–Pt is promising to function as cathodes for large scale high performance aqueous-cathode MFCs.

Acknowledgements

This work was partially supported by the King Abdullah University of Science and Technology (KAUST) Investigator Award (No. KUS-l1-001-12). JM acknowledges support from the National Defense Science and Engineering and National Science Foundation graduate research fellowships. YY and XX acknowledge support from the Stanford Graduate Fellowship.

Notes and references

1 B. E. Logan, *Nat. Rev. Microbiol.*, 2009, **7**, 375–381.
2 B. E. Logan, B. Hamelers, R. A. Rozendal, U. Schrorder, J. Keller, S. Freguia, P. Aelterman, W. Verstraete and K. Rabaey, *Environ. Sci. Technol.*, 2006, **40**, 5181–5192.
3 K. Rabaey and W. Verstraete, *Trends Biotechnol.*, 2005, **23**, 291–298.
4 H. Liu, R. Ramnarayanan and B. E. Logan, *Environ. Sci. Technol.*, 2004, **38**, 2281–2285.
5 F. Zhao, F. Harnisch, U. Schrorder, F. Scholz, P. Bogdanoff and I. Herrmann, *Environ. Sci. Technol.*, 2006, **40**, 5193–5199.
6 Y. Zuo, S. Cheng and B. E. Logan, *Environ. Sci. Technol.*, 2008, **42**, 6967–6972.
7 S. Oh, B. Min and B. E. Logan, *Environ. Sci. Technol.*, 2004, **38**, 4900–4904.
8 E. HaoYu, S. Cheng, K. Scott and B. Logan, *J. Power Sources*, 2007, **171**, 275–281.
9 K. Rabaey and J. Keller, *Water Sci. Technol.*, 2008, **57**, 655–659.
10 R. A. Rozendal, H. V. M. Hamelers, K. Rabaey, J. Keller and C. J. N. Buisman, *Trends Biotechnol.*, 2008, **26**, 450–459.
11 J. R. Kim, S. H. Jung, J. M. Regan and B. E. Logan, *Bioresour. Technol.*, 2007, **98**, 2568–2577.
12 B. E. Logan, C. Murano, K. Scott, N. D. Gray and I. M. Head, *Water Res.*, 2005, **39**, 942–952.
13 B. Min, J. R. Kim, S. E. Oh, J. M. Regan and B. E. Logan, *Water Res.*, 2005, **39**, 4961–4968.
14 B. K. Min, S. A. Cheng and B. E. Logan, *Water Res.*, 2005, **39**, 1675–1686.
15 S. E. Oh and B. E. Logan, *Appl. Microbiol. Biotechnol.*, 2006, **70**, 162–169.
16 X. Cao, X. Huang, P. Liang, K. Xiao, Y. Zhou, X. Zhang and B. E. Logan, *Environ. Sci. Technol.*, 2009, **43**, 7148–7152.
17 S. Cheng, H. Liu and B. E. Logan, *Electrochem. Commun.*, 2006, **8**, 489–494.
18 J. R. Kim, G. C. Premier, F. R. Hawkes, R. M. Dinsdale and A. J. Guwy, *J. Power Sources*, 2009, **187**, 393–399.
19 Y. Zuo, S. Cheng, D. Call and B. E. Logan, *Environ. Sci. Technol.*, 2007, **41**, 3347–3353.
20 C. Wang, M. Waje, X. Wang, J. M. Tang, R. C. Haddon and Y. S. Yan, *Nano Lett.*, 2004, **4**, 345–348.
21 S. Takenaka, H. Matsumori, H. Matsune, E. Tanabe and M. Kishida, *J. Electrochem. Soc.*, 2008, **155**, B929–B936.
22 E. J. Taylor, E. B. Anderson and N. R. K. Vilambi, *J. Electrochem. Soc.*, 1992, **139**, L45–L46.

23 L. Hu, M. Pasta, F. L. Mantia, L. Cui, S. Jeong, H. D. Deshazer, J. W. Choi, S. M. Han and Y. Cui, *Nano Lett.*, 2010, **10**, 708–714.
24 L. B. Hu, J. W. Choi, Y. Yang, S. Jeong, F. La Mantia, L. F. Cui and Y. Cui, *Proc. Natl. Acad. Sci. U. S. A.*, 2009, **106**, 21490–21494.
25 D. S. Hecht, L. Hu and G. Gruner, *Curr. Appl. Phys.*, 2007, **7**, 60–63.
26 X. Xie, L. Hu, M. Pasta, G. F. Wells, D. Kong, C. S. Criddle and Y. Cui, *Nano Lett.*, 2010, **11**, 291–296.
27 K. Saminathan, V. Kamavaram, V. Veedu and A. M. Kannan, *Int. J. Hydrogen Energy*, 2009, **34**, 3838–3844.
28 A. N. Golikand, M. Asgari, E. Lohrasbi and M. Yari, *J. Appl. Electrochem.*, 2009, **39**, 1369–1377.
29 D. V. P. Sanchez, P. Huynh, M. E. Kozlov, R. H. Baughman, R. D. Vidic and M. Yun, *Energy Fuels*, 2010, **24**, 5897–5902.
30 F. Zhao, F. Harnisch, U. Schroder, F. Scholz, P. Bogdanoff and I. Herrmann, *Electrochem. Commun.*, 2005, **7**, 1405–1410.
31 S. Cheng, H. Liu and B. E. Logan, *Environ. Sci. Technol.*, 2006, **40**, 364–369.
32 F. Zhang, S. A. Cheng, D. Pant, G. Van Bogaert and B. E. Logan, *Electrochem. Commun.*, 2009, **11**, 2177–2179.
33 P. Aelterman, M. Versichele, E. Genettello, K. Verbeken and W. Verstraete, *Electrochim. Acta*, 2009, **54**, 5754–5760.
34 L. Deng, M. Zhou, C. Liu, L. Liu, C. Y. Liu and S. J. Dong, *Talanta*, 2010, **81**, 444–448.